PROCEEDINGS OF SCIENCE

A *Fermi* Large Area Telescope analysis unveils possible gamma-ray emission in magnetic cataclysmic variable systems and highly magnetised isolated white dwarfs.

Spencer. T. Madzime[a,*] **and P.J. Meintjes**[a]

[a] *University of the Free State,*
205 Nelson Mandela Dr, Park West, Bloemfontein, South Africa

E-mail: tsmadzime@gmail.com, MeintjPJ@ufs.ac.za

We searched for gamma-ray emission from magnetic cataclysmic variable (MCV) systems, and highly magnetised isolated white dwarfs, using the data observed by the *Fermi* Large Area Telescope (LAT). A total of 75 sources (19 polars, 24 intermediate polars, 6 solitary white dwarfs, 3 double white dwarfs, 18 DQ white dwarfs, 3 DQ Hers, and 2 white dwarf pulsars) were analysed, with a primary focus on those displaying strong magnetic activity and having short orbital periods or white dwarfs with short spin periods. The preliminary results of binned-likelihood analysis in the energy range 0.05-20 GeV revealed 28 sources above the LAT detection level, indicating the presence of gamma-ray emission in these systems. The search for periodic emission in the same energy range in ZTF J153932.16+502738.8 and SDSS J103655.39+652252.2 reveals gamma-ray emissions modulated to the orbital period (6.91 minutes) of ZTF J153932.16+502738.8, with a significance of 5.3 σ, and pulses nearly synchronised with a period of 1115.64751 seconds in SDSS J103655.39+652252.2, with a significance of 5.4 σ. This study provides observational evidence that MCVs with short spin/orbital periods are potential gamma-ray sources. The observed gamma-ray signals provide valuable insights into the underlying physical processes at work in these enigmatic binary systems such as particle acceleration and gamma ray production.

High Energy Astrophysics in Southern Africa 2023 - HEASA2023
5 September - 9 September 2023
Mtunzini, KwaZulu-Natal, South Africa

*Speaker

PoS(HEASA2023)020

1. Introduction

The study explores potential gamma-ray emission from a diverse sample of 75 sources, including polars, intermediate polars, solitary white dwarfs, DQ white dwarfs, DQ Hers, and white dwarf pulsars. Special attention is given to sources with strong magnetic fields and short orbital or spin periods. Theoretical investigations into rapidly rotating and highly magnetised white dwarfs suggest their capability to accelerate particles to energies on the order of Tera electron Volt (TeV) (e.g., [1–3]). These compact objects may display soft gamma-ray emission, akin to processes observed in magnetars, soft gamma-ray repeaters (SGRs), and anomalous X-ray pulsars (AXPs) [4–7]. Magnetars, characterised by strong magnetic fields, are solitary neutron stars powered by magnetic energy. For an in-depth exploration of rotation-powered white dwarfs, Meintjes et al. [1] demonstrate the crucial role of curvature radiation in producing gamma-ray photons with energies below $\epsilon_\gamma \leq 50\,\mathrm{GeV}$ in the proximity of the white dwarf surface.

Polars are also known as AM Her system due to their similarity to AM Herculis binary system, are a subclass of MCVs that have strong magnetic fields. This distinct class is marked by a magnetic white dwarf as the primary star, accompanied by a less massive secondary star (red dwarf). The magnetic influence of the white dwarf disrupts the formation of an accretion disc, causing material to directly flow onto the white dwarf's magnetic poles. This unique mechanism results in the emission of polarised light (e.g., optical-IR) and synchronised spin and orbital period [8, 9]. Characterising features of polar systems include X-ray emission [10], optical spectra with high excitation levels, and notable stability in both X-ray and optical periods seen in their light curves.

Intermediate polars form a subset within MCVs and exhibit magnetic fields of lesser intensity compared to polars. Their distinctive features include a magnetic white dwarf as the primary star, accompanied by a secondary star (red dwarf). Although the white dwarf's magnetic field disrupts the accretion disc, it lacks the strength to direct material onto the magnetic poles directly or synchronise spin and orbital periods. Instead, material flows onto the equator of the white dwarf, forming an accretion belt. These intermediate polars are notable for their X-ray emission (e.g., [10, 11]), originating from high-velocity particles in the accretion stream creating shocks upon falling onto the white dwarf's surface. As these particles decelerate and cool before reaching the white dwarf surface, bremsstrahlung X-rays are produced, potentially absorbed by gas surrounding the shock region.

Isolated white dwarfs are white dwarfs that exist independently, not forming part of a binary system. They originate from the evolutionary process of stars with masses ranging between 0.5 and 8 solar masses, as described by Croswell [12]. As these stars deplete their fuel, they shed their outer layers, and the remaining core undergoes gravitational contraction to give rise to a white dwarf. As a result of the high internal temperature that can reach values of $\sim 10^7$ K the helium, carbon and oxygen may be ionised resulting in a huge population of free electrons that will be squeezed so closely together that they resist further compression. There is also another alternative formation channel of rapidly rotating isolated white dwarfs with strong magnetic fields, which is linked to interactions within closely orbiting binary star systems [13, 14]

DQ Herculis stars constitute a subset of MCVs featuring a magnetic white dwarf as the primary star and a secondary star (red dwarf). Their distinguishing feature lies in the manifestation of carbon emission lines in their spectra, believed to result from the accretion of carbon-rich material onto the

white dwarf. These stars are recognised for their X-ray emission [15], and exhibit spectra with high excitation levels. The stability of optical and X-ray pulsations in the light curves of DQ Herculis stars is noteworthy.

White dwarf pulsars represent a category of MCVs featuring a highly magnetised white dwarf as the primary star and a secondary star (red dwarf). White dwarf pulsars exhibits pulsar-like behaviour. The pulsar-like behaviour arises from the intense magnetic field of the white dwarf, causing emission of radiation and periodic pulses of light. This pulsar-like activity is analogous to what is observed in neutron star pulsars, though the underlying mechanisms may differ due to the contrasting nature of white dwarfs and neutron stars. Their distinguishing feature lies in the presence of synchronised pulsations observed in X-ray and/or optical and/or radio emission [16, 17], which are thought to arise from the rotational motion of the white dwarf. In 2017, researchers affiliated with the University of Warwick discovered AR Scorpii the first object to be classified as a white dwarf pulsar [18]. AR Scorpii exhibits strong linear polarisation, reaching up to 40%, which varies with both the white dwarf's spin period and the beat period resulting from its orbital motion [19]. This is accompanied by low-level circular polarisation. The mechanism driving these phenomena involves magnetic interactions between the stars and synchrotron radiation emitted from the white dwarf.

White dwarfs exhibiting spectroscopic evidence of carbon, identified through the presence of neutral carbon lines or molecular C_2 Swan bands, are classified as DQ white dwarfs (e.g., [20–24]). What makes them unique is their carbon-rich atmospheres, which are different from most other white dwarfs that have helium in their outer layers. Some of these DQ white dwarfs also have weak to moderate magnetic fields, and a few of them even change in brightness over time (e.g., [25]). These stars are not too hot or too cold, with temperatures ranging from around 18 000 to 24 000 degrees Kelvin. It has been shown (e.g. [1] and references therein) that the pressure scale height of an isolated white dwarf with surface temperature of the order of 20 000 K is approximately 10 km, which implies a vacuum region above that where field aligned potentials can be maintained to accelerate charged particles to very high energies (see [1] for a detailed discussion). It has been shown ([1]) that if curvature radiation is considered as the dominant radiation mechanism, the curvature loss time scale sets an upper limit for the gamma-ray energy to approximately $\epsilon_c \leq 50$ GeV. This upper limit will influence our search range for both pulsed and unpulsed gamma-ray emission in the LAT data. The sources of interest are MCVs with high magnetic fields and highly magnetised isolated white dwarfs with short orbital/spin periods. It has been shown by Meintjes et al. [1] that these attributes are conducive to particle acceleration to relativistic energies. Detecting gamma-ray emissions from these sources will enhance our understanding of the mechanisms involved as well as the conditions under which they can function. This paper is organised as follows: We begin with a discussion on the acquisition and analysis of LAT data, followed by the presentation of preliminary results. The paper concludes with a discussion and conclusions section.

2. Observation & Analysis of LAT data.

Recent gamma-ray studies showed that AE Aquarii [26, 27] and AR Scorpii [28] are possible gamma-ray sources. The theoretical framework by Meintjes et al. [1] for fast rotating, highly magnetised white dwarfs ($B_* \geq 10^6$ G), suggests particle acceleration to highly relativistic energy and

possible gamma-ray emission due to curvature radiation. We therefore, searched in the optical/X-ray catalogues for sources that falls within the same class and those that have high magnetic fields and short spin/orbital period since these are the main attributes for particles acceleration to relativistic energies. We compiled a total sample of 75 sources, including polars, intermediate polars, solitary white dwarfs, DQ white dwarfs, DQ Hers, and white dwarf pulsars. The analysis considered LAT gamma-ray photon events received between August 4, 2008, at 15:43:36 and June 30, 2023, at 05:21:17. This investigation was carried out employing the Fermi Science Tools software packages (version v11r0p5). The response functions used for the analysis are the P8R3_SOURCE_V2_v1 set, and events corresponding to the source class were selected, specifically using event class (evclass=128) and FRONT+BACK event type (evtype=3). Photon events were collected within a 10-degree region of interest (ROI) centred on the source of interest. This selection accounted for the point spread function (PSF) characteristics of the LAT instrument (e.g., [29, 30]). To minimise contamination from photons generated by cosmic-ray interactions with the atmosphere, a zenith angle cut was applied at 90 degrees. Binned maximum likelihood [31] analyses were performed within the energy ranges 50 MeV-20 GeV and 0.1-500 GeV utilising the routine *gtlike/pyLikelihood*.

The LAT only considers events from the front in the energy range 0.1-100 GeV for first time detection. This helps minimise the risk of false detections because events under 100 MeV might mostly consist of background photons. However, this method could pose a challenge for sources emitting soft gamma rays. Therefore, we searched for potential pulsed gamma-ray signals in LAT data to confirm our findings obtained through binned-likelihood analysis. Our approach involved using the Rayleigh test and Fermi plug-in [32], utilising the TEMPO2 [33] radio timing analysis tool. LAT photon events within the energy range of 50 MeV-20 GeV were considered, extracted from ROI with a 0.6° radius around each source. We employed the LAT event selection process *gtselect* and *gmktime* to choose all events related to the source of interest. The *gtpsearch* routine in Fermi tools (version 10) was then used to fold photon events using the Rayleigh folding analysis algorithm and published ephemeris. Additionally, data were phased using the peak period from *gtpsearch* and the appropriate ephemeris through the Fermi plug-in. The gtpsearch routine within the Fermi science tools (version v10), along with Fermi plugin, incorporate inherent functionalities for executing barycentric correction. Consequently, we provided the necessary parameters (such as source position and spacecraft file) to facilitate the execution of the correction process.

3. Results

Initial binned-likelihood analysis of the LAT data in the energy range 0.1-500 GeV revealed gamma-ray emissions with soft count spectrum, which implied possible emission in 28 sources. Inspecting the counts spectrum revealed possible counts in the energy range 0.1-20 GeV. Therefore, we selected events in the energy range 50 MeV-20 GeV, and conducted binned-likelihood analysis. The results of 28 sources which showed test statistics above the LAT detection threshold (TS=25) are presented in Table 1. The first column of the table lists the name of the source, followed by the associated test statistic (TS), indicating the significance level (significance = $\sqrt{TS}\,\sigma$) of each source. The third column presents the number of predicted counts (Npred). Additionally, the table includes integral flux and its error, measured in the units of $photons\ cm^{-2}s^{-1}$. These statistics provide a baseline to infer gamma-ray emissions and the significance levels associated with each

source. The search for pulsed emission modulated at the orbital or spin period of these sources were also conducted using the Rayleigh test, TEMPO2 and the Fermi plugin. Here photon events were selected from a ROI of 0.6 degrees. Due to lack of space, we will present the Rayleigh test spectrum, H-test spectrum, and light curve of only two sources (ZTF J153932.16+502738.8 and SDSS J103655.39+652252.2), while more detailed analysis discussions will be presented elsewhere. The phased light curve, Rayleigh test spectrum, and H-test spectrum of these two sources reveal evidence of pulsed emission at the orbital/spin period.

Name	**TS**	**Npred**	**Integral Flux** $[photon\ cm^{-2}s^{-1}]$	**Flux Error** $[photon\ cm^{-2}s^{-1}]$
SDSS J141126.20+200911.1	130	4613	1.05×10^{-8}	9.30×10^{-10}
NLTT 12758	66	3048	7.34×10^{-9}	9.87×10^{-10}
CTCV J2056-3014	53	3480	7.84×10^{-9}	1.12×10^{-9}
EF Eri	42	2187	4.89×10^{-9}	7.78×10^{-10}
PG 1031+234	59	2809	6.64×10^{-9}	9.42×10^{-10}
KPD 0005+5106	33	3253	5.65×10^{-9}	1.10×10^{-9}
SDSS J124058.03-015919.2	66	3474	9.14×10^{-9}	1.14×10^{-9}
EXO 023432-5237.3	79	3635	6.92×10^{-9}	8.08×10^{-10}
SDSS J124043.01+671034.68	131	4976	7.43×10^{-9}	6.85×10^{-10}
GD 362	122	5017	8.99×10^{-9}	8.35×10^{-10}
SDSS J142625.71+575218.3	73	3722	5.90×10^{-9}	7.22×10^{-10}
eRASSU J191213.9-441044	43	3609	7.48×10^{-9}	1.21×10^{-9}
ZTF J153932.16+502738.8	51	2798	4.68×10^{-9}	6.99×10^{-10}
SDSS J103655.39+652252.2	56	3962	1.86×10^{-8}	1.04×10^{-10}
PG 1658+441	27	2521	4.15×10^{-9}	7.88×10^{-10}
E1405-451	37	3860	7.80×10^{-9}	1.43×10^{-9}
SDSS J184037.78+642312.3	63	4109	6.08×10^{-9}	7.43×10^{-10}
GD 356	61	2488	4.41×10^{-9}	6.16×10^{-10}
CE Gru	27	1462	3.59×10^{-9}	7.75×10^{-10}
BL Hyi	33	1502	3.32×10^{-9}	6.40×10^{-10}
CV Hyi	53	2939	5.86×10^{-9}	9.08×10^{-10}
EU UMa	28	2222	4.90×10^{-9}	1.03×10^{-9}
UW Pic	87	4515	8.57×10^{-9}	9.80×10^{-10}
RS Cae	26	2255	4.28×10^{-9}	8.48×10^{-10}
MT Dra	47	3088	5.19×10^{-9}	5.30×10^{-10}
MQ Dra	30	2314	3.75×10^{-9}	7.40×10^{-10}
AR UMa	30	2037	3.91×10^{-9}	8.09×10^{-10}
EV UMa	36	1581	2.95×10^{-9}	5.57×10^{-10}

Table 1: The statistics presented in this table were obtained from analysing the LAT data in the energy range 50 MeV-20 GeV. First column is the name of the source, followed by TS, and the Npred is presented in the third column. The integral flux and error are in the units of $photon\ cm^{-2}s^{-1}$.

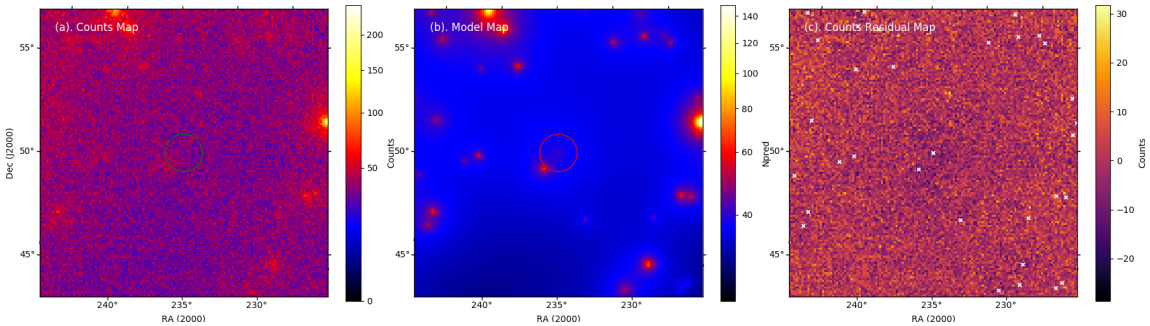

Figure 1: Displayed on the left is the observed counts map of the sources in the ROI of ZTF J153932.16+502738.8, the middle is the model counts map, and in the last panel is the residual map. The predicted counts of significant sources included in the model are shown in the model map. The residual map displays the goodness of the fit, and the crosses in this map indicate the location of sources in the ROI. If there is a huge difference between predicted counts and observed counts the effect will be seen as negative or positive counts at the location where counts are overestimated/underestimated.

3.1 ZTF J153932.16+502738.8

ZTF J153932.16+502738.8 comprises a double binary white dwarf exhibiting a remarkably short orbital period of 6.91 minutes [34]. This binary system manifests as both an eclipsing binary and a double-lined spectroscopic binary. The system consists of two white dwarfs, with one exhibiting a significantly higher temperature than its counterpart. Specifically, the hotter white dwarf boasts an effective temperature of 48900 K, whereas the other white dwarf is notably cooler, with a temperature below 10000 K. There exists the possibility of these stars merging into a singular entity within the next 130000 years, or alternatively, they might undergo separation if mass transfer occurs between them. The system's estimated distance from Earth is approximately 2.3 kiloparsecs. Notably, the orbital period of the system is on a diminishing trajectory at a rate of 2.373×10^{-11} seconds per second, indicating a characteristic timescale of 210000 years before the two white dwarfs merge.

We searched for possible steady gamma-ray emission and periodic oscillations in the energy range 50 MeV-20 GeV. The observed counts map, model counts map, and residual map of the source ZTF J153932.16+502738.8 are illustrated in Figure1. In the model map, all significant sources are included, showing their predicted counts. The residual map indicates the goodness of fit, with extreme negative or positive counts indicating discrepancies between predicted and observed counts. The Rayleigh test power spectrum of ZTF J153932.16+502738.8, H-test plot with TS accumulated from the start of the mission plotted as a function of time, and gamma ray orbital light curve of ZTF J153932.16+502738.8 in the energy range 50 MeV-20 GeV, with photons extracted from a ROI with a radius of 0.6 degrees folded at the orbital period with [34] ephemeris (T_0 = 58305.18278860 MJD) are shown in Figure 2.

3.2 SDSS J103655.39+652252.2

SDSS J103655.39+652252.2 is identified as a DQ white dwarf (e.g., [25]). Recent investigations have revealed photometric variability characterised by a coherent monoperiodic modulation with a period of 1115.64751(67) seconds with a low amplitude of 0.442% ± 0.024%. It is not clear

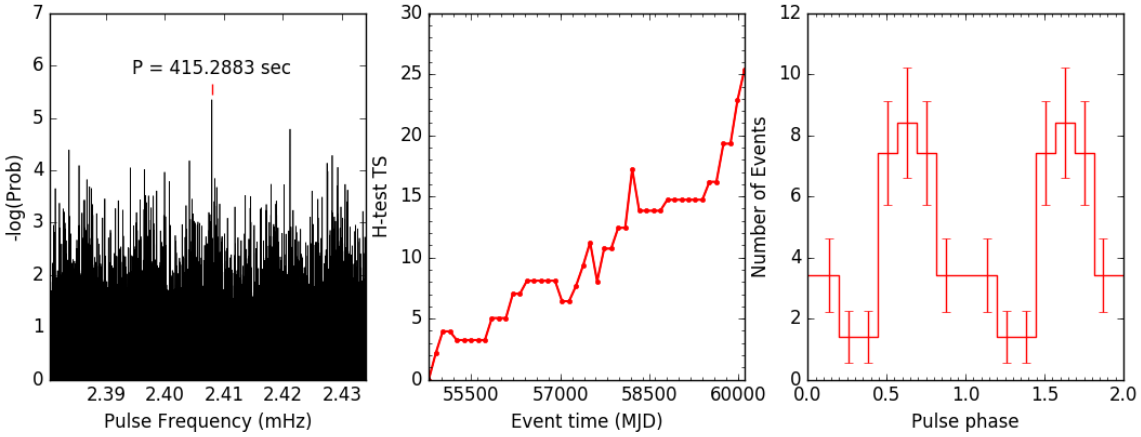

Figure 2: The Rayleigh test power spectrum of ZTF J153932.16+502738.8 shows an indication of pulsed emission close to the 6.9 min orbital period, the H-test plot with TS accumulated from the start of the mission plotted as a function of time indicates that we exceed the threshold of 25 ($5\,\sigma$), and the last panel shows the pulsed gamma-ray light curve of ZTF J153932.16+502738.8 in the energy range 50 MeV-20 GeV, with photons extracted from a ROI with radius of 0.6 degrees folded at the orbital period [34] with ephemeris (T_0 = 58305.18278860 MJD).

whether this period is the spin/orbital period, and no additional periodic modulations are detected with amplitudes exceeding 0.13%. Spectral analysis has further revealed magnetic Zeeman splitting of carbon lines. With an approximate temperature of 15500 K, it possesses a mean magnetic field strength of 3.0 ± 0.2 MG. While the observed variability shares similarities with variable hot DQ white dwarfs, SDSS J1036+6522 exhibits a distinct nearly sinusoidal pulse profile. This sets it apart from other DQ white dwarfs, which typically exhibit significantly asymmetric pulse shapes.

We searched for possible steady gamma-ray and periodic oscillations in the energy range 50 MeV-20 GeV. As before, we show the observed counts map, model counts map, and residual map of the source SDSS J103655.39+652252.2 (see in Figure 3). Figure 4 display the Rayleigh test power spectrum, H-test plot, and gamma-ray light curve of SDSS J103655.39+652252.2, folded at a period of 1115.64751(67) s with the ephemeris provided by Williams et al. [25] (T_0 = 54829.50459000 MJD).

4. Discussion and conclusion

The study of gamma-ray emission from MCVs and highly magnetised isolated white dwarfs, using LAT data, has opened a new window for the study of these enigmatic systems. It has shown that a number of these systems have the required potential to accelerate charged particles to relativistic energies and produce gamma-rays possibly through curvature radiation. The binned-likelihood analysis conducted in the energy range of 0.05-20 GeV resulted in 28 sources that exhibited gamma-ray emission above the LAT detection threshold. The observed pulsed gamma-ray emission from ZTF J153932.16+502738.8 and SDSS J103655.39+652252.2, which are both modulated at the orbital period of these systems, further strengthens our initial hypothesis that the detected emission is unique to the location of the source in the sky. Further studies of these 28 sources, will involve a more detailed analysis which will involve studying their gamma-ray spectral

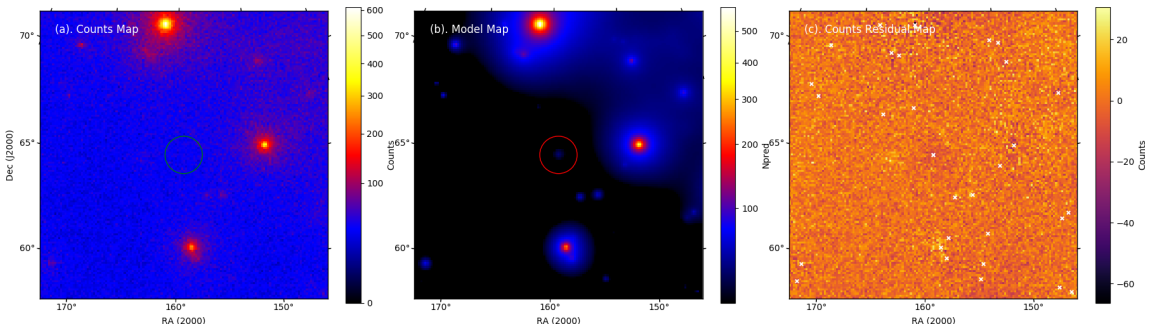

Figure 3: From left to right are the observed counts map of the sources in the ROI of SDSS J103655.39+652252.2, the model counts map with the last panel representing the residual map. The predicted counts of significant sources included in the model are shown in the model map. The residual map displays the goodness of the fit, and the crosses in this map indicate the location of sources in the ROI.

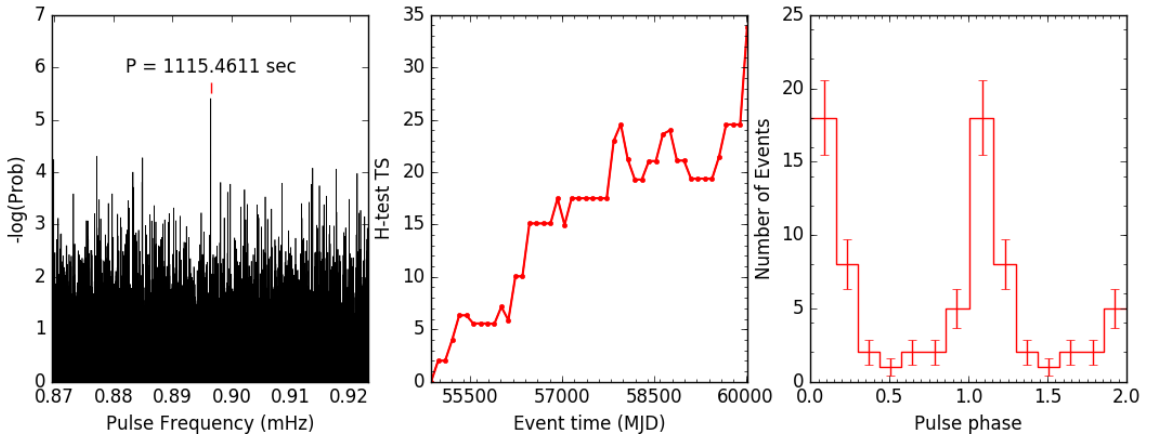

Figure 4: From left to right are the Rayleigh test power spectrum of SDSS J103655.39+652252.2 showing and indication of pulsed emission close to a period of 1115.64751(67) s. The H-test plot in the middle shows the accumulated TS from the start of the mission evolving with time which indicates that we exceed the threshold of 25 (5σ). On the far right right the pulsed gamma-ray phase light curve of SDSS J103655.39+652252.2 in the energy range 50 MeV-20 GeV is presented. The photons had been extracted from a ROI with radius of 0.6 degrees folded at a period of 1115.64751(67) using the Williams et al. [25] ephemeris (T_0 = 54829.50459000 MJD).

properties, and variability on different timescales. In addition, theoretical modelling will be essential for interpreting the observed gamma-ray emission for other subgroups of MCVs. Meintjes et al. [1] showed that due to high magnetic fields and short spin periods in AE Aquarii and AR Scorpii particles can be accelerated to relativistic energies. Short orbital/spin periods and high magnetic fields are the common factor among all the sources considered. Thus, in future we would like to refine models such as the Unipolar inductor model to explain gamma-ray emission from polar MCVs. It is also necessary to complement gamma-ray observations with multi-wavelength studies, i.e observations in X-ray, optical, and radio wavelengths that can help refine our timing models.

References

[1] P. J. Meintjes, S. T. Madzime, Q. Kaplan and H. J. van Heerden, *Spun-up rotation-powered magnetized white dwarfs in close binaries as possible gamma-ray sources: Signatures of pulsed modulation from ae aquarii and ar scorpii in fermi-lat data*, *Galaxies* **11** (2023) 14.

[2] V. Usov, *Generation of gamma-rays by a rotating magnetic white dwarf*, *Soviet Astronomy Letters* **14** (1988) 258.

[3] K. Kashiyama, K. Ioka and N. Kawanaka, *White dwarf pulsars as possible cosmic ray electron-positron factories*, *Physical Review D* **83** (2011) 023002.

[4] S. Mereghetti, *The strongest cosmic magnets: soft gamma-ray repeaters and anomalous x-ray pulsars*, *The Astronomy and Astrophysics Review* **15** (2008) 225.

[5] V. M. Kaspi, *Soft gamma repeaters and anomalous x-ray pulsars: Together forever*, in *Symposium-International Astronomical Union*, vol. 218, pp. 231–238, Cambridge University Press, 2004.

[6] M. Malheiro, J. A. Rueda and R. Ruffini, *Sgrs and axps as rotation-powered massive white dwarfs*, *Publications of the Astronomical Society of Japan* **64** (2012) .

[7] J. Coelho and M. Malheiro, *Similarities of sgrs with low magnetic field and white dwarf pulsars*, in *International Journal of Modern Physics: Conference Series*, vol. 18, pp. 96–100, World Scientific, 2012.

[8] B. Warner, *Cataclysmic Variable Stars, Cambridge University Press, Cambridge*. 1995.

[9] G. Chanmugam and A. Ray, *The rotational and orbital evolution of cataclysmic binaries containing magnetic white dwarfs*, *The Astrophysical Journal* **285** (1984) 252.

[10] J. Frank, A. King, D. Raine et al., *Accretion power in astrophysics*. Cambridge university press, 2002.

[11] C. Hellier, *The intermediate polars*, in *International Astronomical Union Colloquium*, vol. 158, pp. 143–152, Cambridge University Press, 1996.

[12] K. Croswell, *Supernova theory exploded by solitary white dwarfs*, 1991.

[13] K. J. Shen, *Every interacting double white dwarf binary may merge*, *The Astrophysical Journal Letters* **805** (2015) L6.

[14] I. Caiazzo, K. B. Burdge, J. Fuller, J. Heyl, S. Kulkarni, T. A. Prince et al., *A highly magnetized and rapidly rotating white dwarf as small as the moon*, *Nature* **595** (2021) 39.

[15] J. Patterson, *The dq herculis stars*, *Publications of the Astronomical Society of the Pacific* **106** (1994) 209.

[16] R. V. Lobato, M. Malheiro and J. G. Coelho, *Magnetars and white dwarf pulsars*, *International Journal of Modern Physics D* **25** (2016) 1641025.

[17] D. A. Buckley, S. B. Potter, P. J. Meintjes, T. R. Marsh and B. T. Gänsicke, *Polarimetric evidence of the first white dwarf pulsar: The binary system ar scorpii*, *Galaxies* **6** (2018) 14.

[18] T. Marsh, B. Gänsicke, S. Hümmerich, F.-J. Hambsch, K. Bernhard, C. Lloyd et al., *A radio-pulsing white dwarf binary star*, *Nature* **537** (2016) 374.

[19] D. Buckley, P. Meintjes, S. Potter, T. Marsh and B. Gänsicke, *Polarimetric evidence of a white dwarf pulsar in the binary system ar scorpii*, *Nature Astronomy* **1** (2017) 0029.

[20] P. Dufour, P. Bergeron and G. Fontaine, *Detailed spectroscopic and photometric analysis of dq white dwarfs*, *The Astrophysical Journal* **627** (2005) 404.

[21] P. Brassard, G. Fontaine, P. Dufour and P. Bergeron, *The origin and evolution of dq white dwarfs: the carbon pollution problem revisited*, in *15th European Workshop on White Dwarfs*, vol. 372, p. 19, 2007.

[22] P. Dufour, J. Liebert, G. Fontaine and N. Behara, *White dwarf stars with carbon atmospheres*, *Nature* **450** (2007) 522.

[23] P. Dufour, G. Fontaine, J. Liebert, K. Williams and D. K. Lai, *Sdss j142625. 71+ 575218.3: the first pulsating white dwarf with a large detectable magnetic field*, *The Astrophysical Journal* **683** (2008) L167.

[24] P. Dufour, G. Fontaine, J. Liebert, G. D. Schmidt and N. Behara, *Hot dq white dwarfs: Something different*, *The Astrophysical Journal* **683** (2008) 978.

[25] K. A. Williams, D. E. Winget, M. H. Montgomery, P. Dufour, S. O. Kepler, J. J. Hermes et al., *Photometric variability in a warm, strongly magnetic dq white dwarf, sdss j103655. 39+ 652252.2*, *The Astrophysical Journal* **769** (2013) 123.

[26] S. Madzime, P. Meintjes, H. van Heerden, K. Singh, D. Buckley, P. Woudt et al., *The detection of pulsed emission at the spin-period of the white dwarf in ae aquarii in meerkat and fermi-lat data*, in *Proceedings of the 8th High Energy Astrophysics in Southern Africa (HEASA2021) Conference, Online*, pp. 13–17, 2021.

[27] S. T. Madzime, *The search for pulsed radio and gamma-ray emission from the cataclysmic variable system ae aquarii using meerkat and fermi-lat data*, Master's thesis, University of the Free State, 2021.

[28] Q. Kaplan, P. Meintjes and H. van Heerden, *Low-power pulsed emission at the spin period of the white dwarf in ar scorpii?*, .

[29] W. Atwood, A. A. Abdo, M. Ackermann, W. Althouse, B. Anderson, M. Axelsson et al., *The large area telescope on the fermi gamma-ray space telescope mission*, *The Astrophysical Journal* **697** (2009) 1071.

[30] W. Atwood, A. Albert, L. Baldini, M. Tinivella, J. Bregeon, M. Pesce-Rollins et al., *Pass 8: toward the full realization of the fermi-lat scientific potential*, *arXiv preprint arXiv:1303.3514* (2013) .

[31] J. R. Mattox, D. Bertsch, J. Chiang, B. Dingus, S. Digel, J. Esposito et al., *The likelihood analysis of egret data*, *The Astrophysical Journal* **461** (1996) 396.

[32] P. S. Ray, M. Kerr, D. Parent, A. Abdo, L. Guillemot, S. Ransom et al., *Precise γ-ray timing and radio observations of 17 fermi γ-ray pulsars*, *The Astrophysical Journal Supplement Series* **194** (2011) 17.

[33] G. Hobbs, R. Edwards and R. Manchester, *Tempo2, a new pulsar-timing package–i. an overview*, *Monthly Notices of the Royal Astronomical Society* **369** (2006) 655.

[34] K. B. Burdge, M. W. Coughlin, J. Fuller, T. Kupfer, E. C. Bellm, L. Bildsten et al., *General relativistic orbital decay in a seven-minute-orbital-period eclipsing binary system*, *Nature* **571** (2019) 528.